High Shape Persistence in Single Polymer Chains Rigidified with Lateral Hydrogen Bonded Networks

Paolo Samorí,[†,§] Christof Ecker,[†] Illdiko Gössl,[†] Pieter A. J. de Witte,[‡] Jeroen J. L. M. Cornelissen,[‡] Gerald A. Metselaar,[‡] Matthijs B. J. Otten,[†,‡] Alan E. Rowan,[‡] Roeland J. M. Nolte,*[,‡] and Jürgen P. Rabe*[,†]

Department of Physics, Humboldt University Berlin, Invalidenstrasse 110, D-10115 Berlin, Germany; and Department of Organic Chemistry, NSR Center, University of Nijmegen, Toernooiveld, 6525 ED Nijmegen, The Netherlands

Received November 7, 2001; Revised Manuscript Received February 13, 2002

ABSTRACT: Exploiting tapping mode−scanning force microscopy (TM−SFM), we characterized single polymeric chains of poly(isocyanodipeptides) (PICs) equilibrated in quasi two-dimensions on the basal plane of mica surfaces. While the average contour length $\langle L \rangle$ of an acid-catalyzed PIC bearing L-alanine-D-alanine methyl ester groups was as high as 5.3 μm, the corresponding Ni-catalyzed product exhibited an $\langle L \rangle$ of 70 nm. With a newly devised method based on the statistical analysis of the curvature of polymeric chains on a length scale up to about 100 nm from SFM images, we determined their persistence length ℓ_p. The measured value of $\ell_p = 76 \pm 6$ nm for both products, independent of the contour length, indicates that the single polymer molecules are very rigid, i.e., even more rigid than the double-stranded DNA. This rigidity is attributed to the helical structure of the polymer backbone and, in particular, to the hydrogen-bonded networks that are present between the alanine moieties in the side chains.

Introduction

The direct probing of the structural and mechanical properties of isolated polymer chains is one of the major challenges in polymer and material science, since the basic molecular properties can be eventually compared to the macroscopic properties of a material. Scanning probe microscopy techniques make it possible to directly access conformational and mechanical properties of single molecules.[1] For instance, macromolecules can be pulled with a scanning force microscopy tip[2] or imaged when equilibrated on a surface.[3] In the latter case, the persistence length of the molecule on a surface can be determined and compared to the persistence length in solution. Such studies have revealed that double-stranded DNA (dsDNA) on mica has a persistence length of 53 nm, which is similar to the value measured in solution.[3] Wider, more complex supramolecular bio-architectures can be even more rigid and have persistence lengths up to a few millimeters. Examples are the tobacco mosaic virus and the microtubuli.[4]

The synthesis of shape persistent abiotic polymeric structures with preprogrammed conformations is of great recent interest.[5] Such architectures can be constructed by designing supramolecular polymers, where the repeat units are held together through noncovalent types of forces.[6] Alternatively, conventional polymers, where the repeat units are covalenty linked, can be provided with appropriate side-chain functionalities which give additional rigidity to the main chains, e.g., using sterically demanding dendrons,[7] or moieties forming hydrogen-bonded networks.[8]

Among rodlike conventional polymers, poly(isocyanides) (PIC)[9−12] (Figure 1a) are peculiar since their backbones, when functionalized with sterically demanding side chains, adopt a 4_1 helical conformation (four repeats per turn, Figure 1b) which accounts for the relatively high stiffness of the polymer.[9] We decided to focus on a PIC bearing L-alanine-D-alanine methyl ester side groups. Solution studies have revealed that the amide moieties in these pendant dipeptides self-associate into four hydrogen-bonded networks which are oriented parallel to the main chain of the polymer (Figure 1c).[13] This effect is expected to play an important role for the stiffness of the overall chain which needs to be quantified.

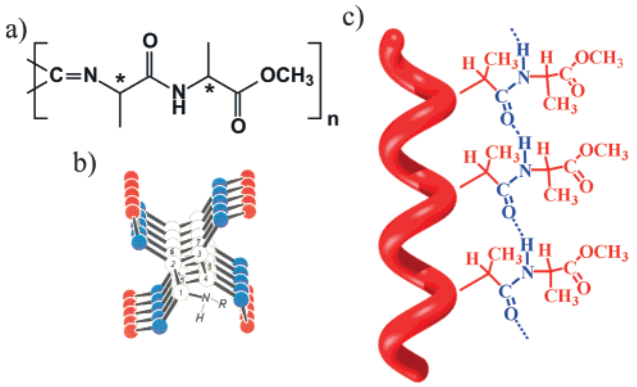

Figure 1. (a) Structure of poly(isocyano-L-alanine-D-alanine methyl ester). (b) Scheme of 4_1-helix. (c) Hydrogen-bonded array within the side chains of the polymer.

We describe here a tapping mode−scanning force microscopy (SFM)[14] investigation of long and stiff isolated poly(isocyanodipeptides) chains equilibrated on the basal surface of mica. The analysis of the SFM data allows us to characterize the stiffness of individual polymer chains by determining their persistence length. We compare the properties of the poly(isocyanodipeptide)s synthesized either with a Ni(II) salt or trifluoroacetic acid as the catalyst.

* Corresponding authors. J.P.R. E-mail: rabe@physik.hu-berlin.de. Fax: +49-30-20937632. R.J.M.N. E-mail: nolte@sci.kun.nl. Fax: +31-243652929.
[†] Humboldt University Berlin.
[‡] University of Nijmegen.
[§] Present address: Instituto per la Sintesi Organica e la Fotoreattività, C.N.R. Bologna, via Gobetti 101, 40129 Bologna, Italy.

10.1021/ma011946b CCC: $22.00
Published on Web 05/16/2002

Methods

Sample Preparation and SFM Imaging. The polymerization reaction was carried out employing either $Ni(ClO_4)_2 \cdot 6H_2O$ (leading to PIC−Ni)[15a] or trifluoroacetic acid (leading to PIC−H)[15b] as catalyst.

PIC solutions of different concentrations in $CHCl_3$ were spin-coated onto freshly cleaved muscovite mica surfaces. The morphologies of the dry thin films were analyzed by means of tapping mode SFM using a Nanoscope IIIa instrument[16] operating at room temperature in an air environment with a relative humidity of 50−70%. Height and phase images were recorded with microfabricated silicon nanoprobes (length 125 μm and width 30 μm) having a spring constant between 17 and 64 N/m,[16] using scan rates of 1−3 lines/s and a resolution of 512 × 512 pixels. The set-point for the tapping mode operation was chosen as high as possible ("light tapping") in order to minimize the interaction forces between the tip and the sample surface.

The data processing was performed with a home-developed software[17] which allowed the analysis of the contours of the macromolecules after visualization by SFM. The molar masses were determined from the distribution of the contour lengths (L) by calculating the number-average (M_n) and the mass-weighted average (M_w), respectively. Since the distribution of L is not Gaussian, the error bar on $\langle L \rangle$ was evaluated with the bootstrapping procedure, provided the data set was large enough (as in the case of PIC−Ni). From the original set of L_i comprising 212 analyzed molecules, a new vector consisting of again 212 data points is created by randomly choosing 212 values L_i' among the original set of L_i, allowing also a multiple selection of a L_i. This procedure is repeated 1000 times, and for each step the average value $\langle L_i' \rangle$ is calculated. From the width of the distribution of the average values $\langle L_i' \rangle$ the error bar on the average contour length can be estimated.[18] For PIC−H only a relatively small number of data points was collected; therefore, it was not possible to use the bootstrapping procedure and the error bars were estimated, approximating the distribution as Gaussian. In this case the error bar on $\langle L \rangle$ is

$$\sqrt{\frac{\sum_{i=1}^{N}(\langle L \rangle - L_i)^2}{N-1}}$$

if N is the number of analyzed molecules. To estimate the error of this procedure, the error bar for $\langle L \rangle$ of the PIC−Ni samples was determined both with the bootstrapping procedure and with the approximation of a Gaussian distribution, giving numbers of ±3 nm and ±5 nm, respectively.

Determination of the Persistence Lengths. According to the "wormlike chain model", also known as the "Kratky−Porod model",[19,20] for semiflexible chains the persistence length ℓ_p is the length over which the memory of the initial orientation of the chain is maintained. The shape persistence of polymeric chains can be analyzed by determining the statistical fluctuations in the curvatures of many single macromolecules equilibrated on a surface. These fluctuations can be visualized by SFM[3] or electron microscopy[21] and permit to determine the persistence length of the chains with a high precision.

For a polymer chain in two dimensions, the angle $\theta(\ell)$ between the tangents at two points located a distance ℓ apart along the contour can be described by the following probability distribution function:[3]

$$\mathcal{P}(\theta(\ell)) = \sqrt{\frac{\ell_p}{2\pi\ell}}\, e^{-[\ell_p\theta^2(\ell)]/2\ell}$$

This is a normal distribution characterized by a mean value

$$\langle \theta(\ell) \rangle = \int_{-\infty}^{\infty} d\theta\, (\ell)\mathcal{P}(\theta(\ell)) = 0$$

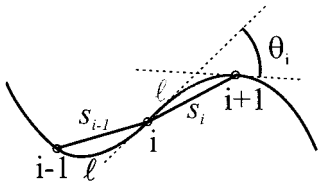

Figure 2. Schematic representation of the determination of θ_i along a chain section of length ℓ (in gray) which goes from i to $i + 1$.

and the variance

$$V[\theta(\ell)] = \int_{-\infty}^{\infty} d\theta\, (\ell)(\langle \theta(\ell) \rangle - \theta(\ell))^2 \mathcal{P}(\theta(\ell)) = \frac{\ell}{\ell_p} \qquad (1)$$

A simple way to represent the contour of the chain is to draw a series of consecutive straight segments connecting points, which are located at constant contour lengths ℓ apart (Figure 2). One can then construct a set of θ_i values from the angles between the tangents at i and $i + 1$. If ℓ is chosen to be sufficiently small, namely $\ell \ll \ell_p$, the length of the straight segments s connecting the points i and $i + 1$ approaches ℓ, and eq 1 becomes

$$V[\theta_i] = \frac{s}{\ell_p} \qquad (2)$$

Using eq 2, the persistence lengths can be determined with a high precision from the SFM images as long as the image resolution allows one to accurately digitize the data with $\ell \ll \ell_p$.

For determining the persistence length of the chains in a given sample, SFM images were recorded with a resolution of 512 × 512 pixels, with pixel sizes ranging from 1 to 10 nm. The chain images were vectorized by selecting points on the chains which were then connected by straight lines with a length of approximately 5 pixels using a drawing program.[22]

The set of θ_i values was obtained from the tangents in each data point. Since the segment lengths s_i are not constant, the angles θ_i had to be normalized. Because of the proportionality $\langle \theta_i^2 \rangle \propto s$ which is reflected in eq 2, this normalization was carried out by setting $\tilde{\theta}_i \equiv \theta_i/\sqrt{s_i}$ and consequently $\tilde{s}_i = \tilde{s} \equiv 1$.

Equation 2 then becomes

$$V[\tilde{\theta}_i] \cong \frac{1}{\ell_p} \qquad (3)$$

Since the set of measured data θ_i^m was determined with a manual vectorization procedure, it possesses a random error of $\theta_i^m = \theta_i + \varphi_i$. Thus, $V[\tilde{\theta}_i^m]$ will differ from the variance of the exact $\tilde{\theta}_i$, namely $V[\tilde{\theta}_i]$. Assuming the errors to have a normal distribution, the measured variance of the normalized data is $V[\tilde{\theta}_i] + V[\tilde{\varphi}_i]$. Since $V[\tilde{\varphi}_i]$ is independent of $\tilde{s}$, the exact $V[\tilde{\theta}_i]$ can be also calculated by building-up a new chain of different $\tilde{s}_2$. Constructing a set of $\tilde{\theta}_i^{m2}$ values corresponding to a segment length $\tilde{s}_2 = 3 \cdot \tilde{s} = 3$ the true variance amounts to

$$V[\tilde{\theta}_i] = \frac{1}{2}(V[\tilde{\theta}_i^{m2}] - V[\tilde{\theta}_i^{m}]) \qquad (4)$$

The values $V[\tilde{\theta}_i^m]$ and $V[\tilde{\theta}_i^{m2}]$ were calculated for each chain and then averaged weighting the values by the length of the molecule. This latter procedure was used in order to obtain values of the variance that are weighted by the contour length of the chain, rather than by the number of data points collected with the vectorization procedure. Finally, by combination of eqs 2 and 4, one obtains the average value of the persistence length for a given sample:

$$\ell_p = \frac{2}{(V[\tilde{\theta}_i^{m2}] - V[\tilde{\theta}_i^{m}])} \qquad (5)$$

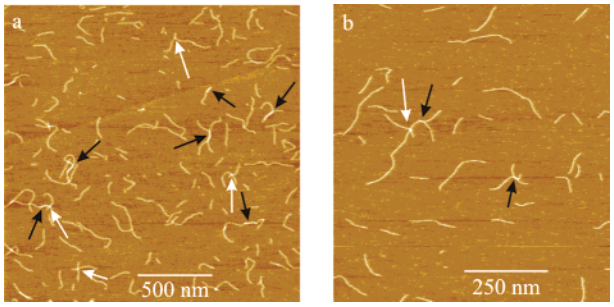

Figure 3. SFM images of a PIC−Ni sample. Film prepared from a chloroform solution containing (a) 0.01 and (b) 0.001 g/L of PIC−Ni. White arrows indicate intersections of separate chains and black ones mark segments consisting of intercoiled chains. Z range: $h = 2$ nm.

Because of the normal distribution of $\tilde{\theta}_i^m$ and $\tilde{\theta}_i^{m2}$, the distribution of $V[\tilde{\theta}_i^m]$ and $V[\tilde{\theta}_i^{m2}]$ can be described using the χ^2-statistics.[23] Taking σ as the confidence interval, one gets $\Delta V[\tilde{\theta}_i^m] = V[\tilde{\theta}_i^m]\sqrt{3/N}$ and $\Delta V[\tilde{\theta}_i^{m2}] = V[\tilde{\theta}_i^{m2}]\sqrt{6/N}$, where N is the number of data samples. Applying the formalism of the Gaussian error propagation the error of $\not{\Delta}_p$ is

$$\Delta\not{\Delta}_p = \sqrt{\frac{3(V[\tilde{\theta}_i^m]^2 + 2V[\tilde{\theta}_i^{m2}]^2)}{N(V[\tilde{\theta}_i^m] - V[\tilde{\theta}_i^{m2}])^2}}$$

Results and Discussion

Single Chain Visualization by SFM. Figure 3 displays SFM images of isolated PIC chains prepared by a nickel(II)-catalyzed polymerization reaction (PIC−Ni). The chains exhibit cross sections that typically are constant along their whole lengths. The fact that the ends and the middle sections of the chains are equal suggests in particular that they consist of single strands. The apparent thickness of the chains, which amounts to 0.30 ± 0.06 nm, is lower than the diameter of the PIC rod which was calculated to be 1.58 nm.[13] This effect has been observed before with different macromolecules adsorbed on surfaces, including dendrimers[24] and filamentous phage fd.[25] It can become dramatic in an atmosphere characterized by a high relative humidity[25] and can be due to the indentation of the macromolecule by the probing SFM tip,[26] the adhesion of the tip to the surface[27] and/or the flattening of the macromolecule on the substrate.[28] A careful analysis of the images in Figure 3 allowed us to distinguish two different types of features with larger thicknesses: (i) intersections between two chains, as indicated by white arrows and (ii) segments consisting of two chains tightly packed one on the top of each other, as marked with black arrows. In both cases, the thicknesses were approximately 1.6−2.0 times those of the single chains. In the second case, the limits in the spatial resolution of the SFM due to the tip convolution did not permit a distinction between segments consisting of chains that are packed one on top of each other and segments composed of intercoiled strands.

SFM images of PICs prepared by the acid-catalyzed polymerization reaction (PIC−H) are shown in Figure 4. Films prepared from 0.01 g/L solutions (Figure 4a) revealed an entangled network of polymer chains coexisting with free-standing single polymer strands. In these two different arrangements the polymer chains exhibited two completely different structures: in the first case topological constraints as a result of the entanglements, marked with the black arrows, caused a tension in the superstructure which did not permit

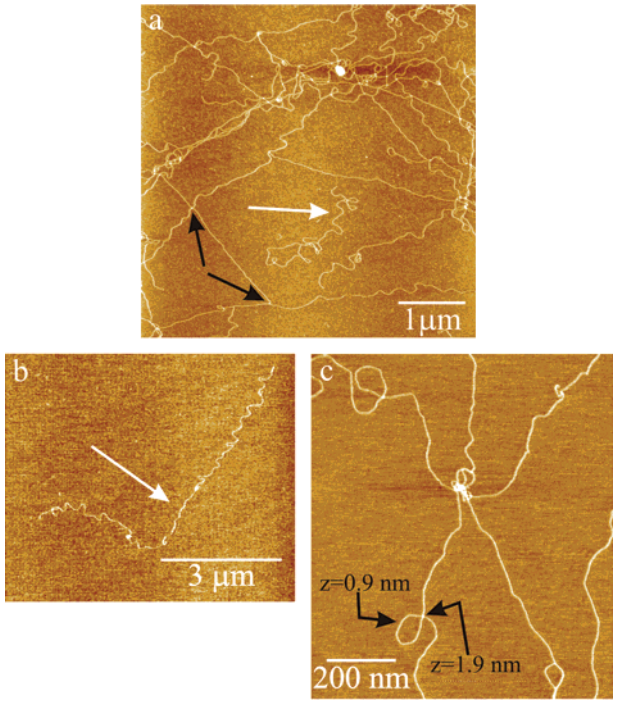

Figure 4. SFM images of PIC−H. (a) Sample prepared from an 0.01 g/L polymer solution in $CHCl_3$ revealing the coexistence of relaxed chains (indicated by the white arrow) and tightened ones (entanglements at the edges are marked with black arrows). (b, c) Spin-coated films prepared from 0.001 g/L polymer solutions in $CHCl_3$ in which isolated chains can be seen. (c) Zoom-in on chain intersections (bottom left) and on wrapped chains (top right). Whereas in the first case the observed thickness is twice that of a single chain, in the latter case this thickness is less than the double value. Z range: (a) $h = 4$ nm; (b) $h = 2$ nm; (c) $h = 4$ nm.

the strands to equilibrate (see also below). In the second case the chains were able to equilibrate up to a length scale of approximately 100 nm on the surface, as indicated by the white arrows in Figure 4, parts a and b (the latter image was taken from a film prepared from a 0.001 g/L solution). As in the case of PIC−Ni, an analysis of the thicknesses of the rods made it possible to identify intersections between two chains and segments consisting of intercoiled or tightly packed chains, besides individual chains on mica with a height of ca. 0.8 nm (Figure 4c).

Contour Length. The quantitative determination of the contour lengths (L) of isolated polymer chains from SFM images[3] allows one to quantify the molar mass distribution of a polymer.[26] The distribution of L for the PIC−Ni samples is shown in Figure 5a. The average contour length was found to be $\langle L \rangle = 70 \pm 3$ nm, which corresponds to a number-average molar mass of $M_n = 118 \times 10^3$ g/mol. From the distribution the polydispersity was calculated to be $M_w/M_n = 1.36 \pm 0.04$, where M_w is the mass average molar mass. The longest measured polymer chain exhibited a contour length of ca. 220 nm. The polymer synthesized by the acid catalyzed polymerization reaction displayed a higher degree of polymerization. The analysis performed on isolated chains such as the ones in Figure 4b, although being limited to only a few tens of strands, revealed the very high value of $\langle L \rangle = 5.3 \pm 1.3$ μm, corresponding to $M_n = 8.94 \times 10^6$ g/mol, and $M_w/M_n = 1.35 \pm 0.7$. In this case the contour length of the longest chain was found to be 12.7 μm !

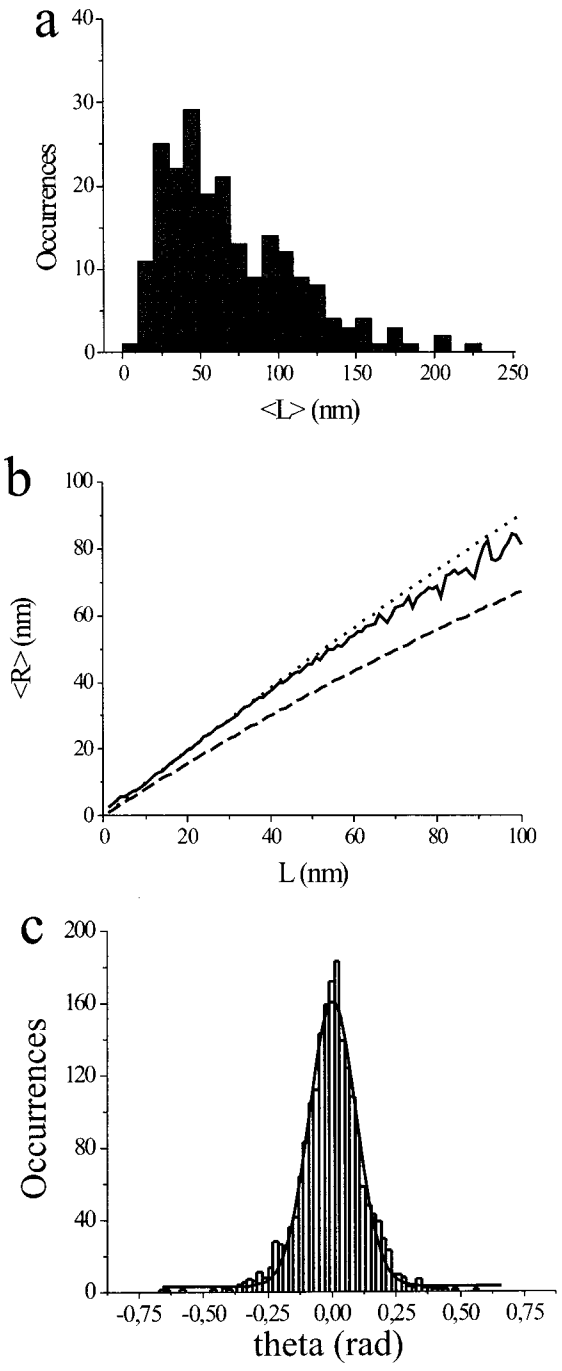

Figure 5. (a) Histograms of the distribution of the contour lengths of PIC−Ni obtained from the SFM images. (b) Evolution of the end-to-end distance vs the contour length. Theoretical function for 2D equilibrated chains (dotted line), 2D trapped chains (dashed line) and experimental results (filled line). (c) Distribution of the θ_i values as determined from the experimental results and the calculated Gaussian function.

Persistence Length. Following the procedure described in the Methods section,[17] the persistence lengths for PIC−Ni and PIC−H were determined to be $\ell_p = 76 \pm 6$ nm and $\ell_p = 76 \pm 5$ nm, respectively. In the latter case, only chains in the relaxed states were selected for the analysis. The remarkable agreement of their persistence lengths reflects the identical chemical structure of both polymers. Furthermore, the good agreement observed for short and long polymer chains indicates that the role played by long-range interactions, i.e., excluded volume effects, is negligible.[29]

It is most important to note that the chains may be physisorbed on the surface in either a kinetically trapped 3D-conformation or a conformation that is in the 2D thermodynamic equilibrium conformation. In the former case, the observed structures resemble the projection on the surface of the conformations attained in solution and reflect the history of the approach of the molecules to the surface. In the latter case the molecules are allowed to search among their accessible states in two dimensions before they are captured in a particular 2D-conformation. As discussed for other macromolecular systems,[3] only for chains which are equilibrated at surfaces in quasi 2D, it is possible from SFM images to evaluate quantitatively the persistence length according to the wormlike chain model, and consequently the 3D mechanical and structural properties of the polymer. Therefore, for our type of investigation it is crucial to be able to differentiate between trapped 3D-conformations and macromolecules equilibrated in quasi 2D. In the present case, this identification was done using two different approaches. In the following part, the data regarding the PIC−Ni samples are presented.

First, according to Rivetti et al.[3] the average end-to-end distance $\langle R \rangle$ of a chain equilibrated in 2D on a surface can be described by

$$\langle R^2 \rangle_{2D-EQ} = 4\ell_p L\left(1 - \frac{2\ell_p}{L}(1 - e^{-L/2\ell_p})\right)$$

whereas for 3D-chains trapped on the surface

$$\langle R^2 \rangle_{2D-TRAPPED} = \frac{4}{3}\ell_p L\left(1 - \frac{\ell_p}{L}(1 - e^{-L/2\ell_p})\right)$$

In Figure 5b $\langle R \rangle$ vs L are plotted for these two functions using the experimentally determined value for $\ell_p = 76 \pm 6$ nm. A good agreement between the experimental data and the calculated curve representing the equilibrated chains in 2D is observed in the range from $L = 0$ nm to $L = 50$ nm. For higher L values, due to the low number of data points, the evolution of $\langle R \rangle = f(L)$ is characterized by larger fluctuations. Nevertheless, a reasonably good agreement between the theoretical curve for the equilibrated chains in 2D and the experimental results is still evident. This not only proves that the chains are equilibrated on the surface, but also represents an independent verification of the determined ℓ_p, according to the wormlike chain model.[3]

Alternatively, in Figure 5c the distribution of the angles θ_i, which for the thermodynamically stable states must be Gaussian,[21] is plotted in the histograms. A good fit to a Gaussian function can be obtained, as confirmed by the value of $\chi^2 = 42.07$ (for 2740 data points sorted in 67 bins) which attests to a confidence of more than 95%.

The two crosschecks described above provide the evidence that for both PIC−Ni and PIC−H the chains are equilibrated on the surface up to a length scale of about 100 nm. Moreover, it is important to note that none of the samples exhibited a preferential orientation of the adsorbed chains with respect to the 3-fold symmetry of the mica substrate. This determination, which has been accomplished by sampling the orientation of each vectorized segment relative to a fixed coordinate system in the given SFM image, revealed a random distribution of the orientations.

Conclusions

We have shown that the recently developed polymers of isocyanodipeptides are extraordinarily stiff macromolecules. To determine the persistence length of synthetic macromolecules, alternatively to the more indirect scattering methods employed in solutions, we have exploited a new versatile method based on SFM visualization of the conformation of isolated macromolecules equilibrated in quasi 2D on a surface. The measured persistence length amounts to 76 ± 6 nm, which is more than 1 order of magnitude larger than the persistence length determined in solutions for a simpler PIC, namely poly(α-phenylethylisocyanide).[10] This indicates that the hydrogen-bonded networks in the side chains of the polymers stabilize the overall polymer structure in line with previous physicochemical studies.[13] Among single chain synthetic polymers the stiffness of our PICs indeed is very high: it is comparable to the one quantified in solutions for poly(γ-benzyl-α,L-glutamate) for which a persistence lengths of ℓ_p = 70 nm was reported,[30] and it is higher than other polymers that are considered to be very rigid, e.g., hyperbranched or dendronized polymers that exhibited a ℓ_p = 50 nm.[7b] Remarkably, our polymer exhibits a persistence length that is even 50% larger than that of dsDNA.[3] Further physicochemical investigations on these extraordinarily stiff macromolecules appear feasible, such as mechano-chemical studies on the elasticity of the chains, which can also be carried out with scanning force spectroscopy[2] or studies using optical tweezers.[31]

Acknowledgment. This work was supported by the EU-TMR project SISITOMAS (project reference FMRX970099), by the European Science Foundation through the SMARTON program, and by the Deutsche Forschungsgemeinschaft (Sfb448 "Mesoskopisch strukturierte Verbundsysteme").

References and Notes

(1) (a) Gimzewski, J. K.; Joachim, C. *Science* **1999**, *283*, 1683−1688. (b) Yazdani, A.; Lieber, C. M. *Nature (London)* **1999**, *401*, 227−230.

(2) (a) Rief, M.; Oesterhelt, F.; Heymann, B.; Gaub, H. E. *Science* **1997**, *275*, 1295−1297. (b) Bustamante, C.; Macosko, J. C.; Wuite, G. J. L. *Nature Rev. Mol. Cell Bio.* **2000**, *1*, 130−136. (c) Fisher, T. E.; Marszalek, P. E.; Fernandez, J. M. *Nat. Struct. Biol.* **2000**, *7*, 719−724. (d) Janshoff, A.; Neitzert, M.; Oberdörfer, Y.; Fuchs, H. *Angew. Chem., Int. Ed.* **2000**, *39*, 3213−3237; *Angew. Chem.* **2000**, *112*, 3346−3374. (e) Samorì, B. *Chem.−Eur. J.* **2000**, *6*, 4249−4255.

(3) Rivetti, C.; Guthold, M.; Bustamante, C. *J. Mol. Biol.* **1996**, *264*, 919−932.

(4) Gittes, F.; Mickey, B.; Nettleton, J. Howard,J. *J. Cell Biol.* ***1993***, *120*, 923−934.

(5) (a) Muthukumar, M.; Ober, C. K.; Thomas, E. L. *Science* **1997**, *277*, 1225−1232. (b) Ober, C. K. *Science* **2000**, *288*, 448−449. (c) Kim, J.; Swager, T. M. *Nature (London)* **2001**, *411*, 1030−1034. (d) Bong, D. T.; Clark, T. D.; Granja, J. R.; Ghadiri, M. R. *Angew. Chem., Int. Ed. Engl.* **2001**, *40*, 988−1011; *Angew. Chem.* **2001**, *113*, 1016−1041. (e) Sellinger, J. V.; Spector, M. S.; Schnur, J. M *J. Phys. Chem. B* **2001**, 105, 7157−7169.

(6) (a) Moore, J. S. Curr. Op. Coll. Interface Sci. **1999**, *4*, 108−116. (b) Semenov, A.; Spatz, J. P.; Möller, M.; Lehn, J.-M.; Sell, B.; Schubert, D.; Weidl, C. H.; Schubert, U. S. *Angew. Chem., Int. Ed. Engl.* **1999**, *38*, 2547−2550; *Angew. Chem.* **1999**, *111*, 2701−2705. (c) Guo, S.; Konopny, L.; Popovitz-Biro, R.; Cohen, H.; Porteanu, H.; Lifshitz, E.; Lahav, M. *J. Am. Chem. Soc.* **1999**, *121*, 9589−9598. (d) Kurth, D. G.; Lehmann, P.; Schütte, M. *Proc. Natl. Acad. Sci. U.S.A.* **2000**, *97*, 5704−5707. (e) Hirschberg, J. H. K. K.; Brunsveld, L.; Ramzi, A.; Vekemans, J. A. J. M.; Sijbesma, R. P.; Meijer, E. W. *Nature (London)* **2000**, *407*, 167−170. (f) Gottarelli, G.; Masiero, S.; Mezzina, E.; Pieraccini, S.; Rabe, J. P.; Samorí, P.; Spada, G. P. *Chem.−Eur. J.* **2000**, *6*, 3242−3248. (g) Barth, J. V.; Weckesser, J.; Cai, C.; Günter, P.; Bürgi, L.; Jeandupeux, O.; Kern, K. *Angew. Chem., Int. Ed.* **2000**, *39*, 1230−1234; *Angew. Chem.* **2000**, *112*, 1285−1288. (h) Gesquière, A.; Abdel-Mottaleb, M. M. S.; De Feyter, S.; De Schryver, F. C.; Schoonbeek, F.; van Esch, J.; Kellogg, R. M.; Feringa, B. L.; Calderone, A.; Lazzaroni, R.; Brédas, J. L. *Langmuir* **2000**, *16*, 10385−10391. (i) Raymo, F. M.; Bartberger, M. D.; Houk, K. N.; Stoddart, J. F. *J. Am. Chem. Soc.* **2001**, *123*, 9264−9267.

(7) (a) Karakaya, B.; Claussen, W.; Gessler, K.; Saenger, W.; Schlüter, A.-D. *J. Am. Chem. Soc.* **1997**, *119*, 3296−3301. (b) Percec, V.; Ahn, C.-H.; Cho, W.-D.; Jamieson, A. M.; Kim, J.; Leman, T.; Schmidt, M.; Gerle, M.; Möller, M.; Prokhorova, S. A.; Sheiko, S. S.; Cheng, S. Z. D.; Zhang, A.; Ungar, G.; Yeardley, D. J. P. *J. Am. Chem. Soc.* **1998**, *120*, 8619−8631. (c) Schlüter, A.-D.; Rabe, J. P. *Angew. Chem., Int. Ed.* **2000**, *39*, 864−883; *Angew. Chem.* **2000**, *112*, 860−880.

(8) Delnoye, D. A. P.; Sijbesma, R.; Vekemans, J. A. J. M.; Meijer, E. W. *J. Am. Chem. Soc.* **1996**, *118*, 8717−8718.

(9) Nolte, R. J. M. *Chem. Soc. Rev.* **1994**, *23*, 11−19.

(10) Green, M. M.; Gross, R. A.; Schilling, F.; Zero, K.; Crosby, C. *Macromolecules* **1988**, *21*, 1839−1846.

(11) Clericuzio, M.; Alagona, G.; Ghio, C.; Salvadori, P. *J. Am. Chem. Soc.* **1997**, *119*, 1059−1071.

(12) Amabilino, D. B.; Ramos, E.; Serrano, J.-L.; Sierra, T.; Veciano, V. *J. Am. Chem. Soc.* **1998**, *120*, 9126−9134.

(13) Cornelissen, J. J. L. M.; Donners, J. J. J. M.; Metselaar, G.; de Gelder, R.; Graswinckel, W. S.; Rowan, A. E.; Sommerdijk, N. A. J. M.; Nolte, R. J. M. *Science* **2001**, *293*, 676−680.

(14) Takano, H.; Kenseth, J. R.; Wong, S. S.; O'Brien, J. C.; Porter, M. D. *Chem. Rev.* **1999**, *99*, 2845−2890.

(15) (a) Cornelissen, J. J. L. M.; Graswinckel, W. S.; Adams, P. J. H. M.; Nachtegaal, G. H.; Kentgens, A. P. M.; Sommerdijk, N. A. J. M.; Nolte, R. J. M. *J. Polym. Sci. A*, **2001**, *39*, 4255−4264. (b) Metselaar, G. A.; Rowan, A. E.; Nolte, R. J. M., in preparation.

(16) Digital Instruments, Santa Barbara, CA.

(17) Ecker, C. Ph.D. Thesis, Humboldt University Berlin, in preparation.

(18) Lunneborg, C. E. *Data analysis by resampling: Concepts and applications*; Brooks-Cole: Pacific Grove, CA, 1999.

(19) Kratky, G.; Porod, G. *Recl. Trav. Chim. Pays-Bas* **1949**, *68*, 1106−1122.

(20) Grosberg, A. Y.; Khokhlov, A. R. *Statistical Physics of Macromolecules*; AIP Press: New York, 1994.

(21) Frontali, C.; Dore, E.; Ferrauto, E.; Gratton, E.; Bettini, A.; Pozzan, M. R.; Valdevit, E. *Biopolymers* **1979** *18*, 1353−1373.

(22) Sketch (http://sketch.sourceforge.org) or Corel Draw version 8.232, Corel Corporation.

(23) Taylor, J. R. *Introduction to error analysis − the study of uncertainties in physical measurements*, University Science Books: Herndon, VA, 1997.

(24) Hierlemann, A.; Campbell, J. K.; Baker, L. A.; Crooks, R. M.; Ricco, A. J. *J. Am. Chem. Soc.* **1998**, *120*, 5323−5324.

(25) Ji, X.; Oh, J.; Dunker, A. K.; Hipps, K. W. *Ultramicroscopy* **1998**, *72*, 165−176.

(26) Prokhorova, S. A.; Sheiko, S. S.; Möller, M.; Ahn, C.-H.; Percec, V. *Macromol. Rapid Commun.* **1998**, *19*, 359−366.

(27) van Noort, S. J. T.; van der Werf, K. O.; De Grooth, B. G.; van Hulst, N. F.; Greve, J. *Ultramicroscopy* **1997**, *69*, 117−127.

(28) (a) Prokhorova, S. A.; Sheiko, S. S.; Mourran, A.; Azumi, R.; Beginn, U.; Zipp, G.; Ahn, C.-H.; Holerca, M. N.; Percec, V.; Möller, M. *Langmuir* **2000**, *16*, 6862−6867. (b) Tang, J.; Li, J.; Wang; C:, Bai, C. *J. Vac. Sci. Technol. B* **2000**, *18*, 1858−1860.

(29) The persistence length is calculated from the correlations between neighboring segments with a length of ca. 1−10 nm. Consequently, the data sampling does not introduce an error in the persistence length measurement of the type discussed in ref 3, paragraph "Excluded Volume".

(30) Jamil, T.; Russo, P. S. *J. Chem. Phys.* **1992**, *97*, 2777−2782.

(31) Bustamante, C.; Smith, S. B.; Liphardt, J.; Smith, D. *Curr. Opin. Struct. Biol.* **2000**, *10*, 279−285.

MA011946B